Rocksalt-type PrO epitaxial thin film as a weak ferromagnetic Kondo lattice

Hirokazu Shimizu,[1] Daichi Oka,[1] Kenichi Kaminaga,[2,3] Daichi Saito,[1] Taku Yamamoto,[1] Nobuto Abe,[1] Noriaki Kimura,[4] Daisuke Shiga,[5] Hiroshi Kumigashira,[5,6] and Tomoteru Fukumura[1,2,7]

[1]*Department of Chemistry, Graduate School of Science, Tohoku University, Sendai 980-8578, Japan*
[2]*Advanced Institute for Materials Research (WPI-AIMR) and Core Research Cluster, Tohoku University, Sendai 980-8577, Japan*
[3]*Department of Applied Chemistry, School of Engineering, Tohoku University, Sendai 980-8579, Japan*
[4]*Department of Physics, Graduate School of Science, Center for Low Temperature Science, Tohoku University, Sendai 980-8578, Japan*
[5]*Institute of Multidisciplinary Research for Advanced Materials, Tohoku University, Sendai 980-8577, Japan*
[6]*Photon Factory, Institute of Materials Structure Science, High Energy Accelerator Research Organization (KEK), Tsukuba 305-0801, Japan*
[7]*Center for Science and Innovation in Spintronics, Organization for Advanced Studies, and Center for Spintronics Research Network Tohoku University, Sendai 980-8577, Japan*

(Received 16 July 2021; revised 11 December 2021; accepted 13 January 2022; published 31 January 2022)

A unique Kondo lattice praseodymium monoxide PrO was synthesized in the form of an epitaxial thin film. The rocksalt-type PrO thin films with a $4f^2 5d^1$ electronic configuration showed metallic conduction with a local resistivity minimum at 7 K as a result of the Kondo effect. In contrast to the other paramagnetic praseodymium monochalcogenides, PrO showed weak ferromagnetism below 28 K, followed by a transition to a more ferromagneticlike phase around 5 K. Emergence of the weak ferromagnetism probably originated from the enhanced $4f$-$4f$ exchange interaction by the short Pr-Pr distance. For the ferromagneticlike phase below 5 K, magnetic hysteresis of the anomalous Hall effect was significantly larger than that of magnetization, probably due to competing magnetic ordering.

DOI: 10.1103/PhysRevB.105.014442

I. INTRODUCTION

In the Kondo lattice, a rich electronic and magnetic phase diagram is generated by the competing interactions between localized $4f$ electrons and itinerant carriers such as the Kondo effect and the Ruderman-Kittel-Kasuya-Yosida (RKKY) interaction [1]. Ce compounds with $4f^1$ electron configuration have been extensively studied as a model system of the Kondo lattice [2,3]. On the other hand, crystallographically highly symmetric Pr compounds with $4f^2$ electron configuration show intriguing properties such as superconductivity with quadrupole ordering [4], anomalous Hall effect without long-range magnetic ordering [5], and non-Fermi-liquid behavior [6], originating from the nonmagnetic ground states [7,8]. Because of rather long neighboring Pr-Pr distances of 4.8–6.8 Å in most of the Pr-based Kondo lattice compounds, indirect exchange interactions via the itinerant electrons govern their physical properties [8]. Accordingly, a unique electronic and magnetic phase diagram is expected for a Pr-based Kondo lattice with shorter Pr-Pr distance that underpins local magnetic interactions such as $4f$-$4f$ exchange interaction and superexchange interaction.

Rocksalt-type rare-earth chalcogenides (*Ch*: O, S, Se, Te) and pnictides (*Pn*: N, P, As, Sb) have short cationic distances, particularly for smaller *Ch* and *Pn* ionic radii. For example, Nd*Ch*, Nd*Pn*, Eu*Ch*, Eu*Pn*, and other compounds show antiferromagnetic to ferromagnetic transition for the smaller *Ch* and *Pn* [9–11], attributed to the $4f$-$4f$ exchange interaction enhanced by the shorter nearest neighbor cation distances [12]. On the other hand, Pr*Ch* and Pr*Pn* were reported to be paramagnetic metals and insulators, respectively, except for weak ferromagnetic PrN [13–15]. Metastable PrO polycrystal with the shortest Pr-Pr distance among Pr*Ch* (3.56 Å) was obtained by high-pressure synthesis and reported to also be paramagnetic, although the negative Weiss temperature implied antiferromagnetic interaction [16].

Recently, it was found that rare-earth monoxide epitaxial thin films can be synthesized by using pulsed laser deposition due to their kinetic growth nature [9,17–21]. In this study, we synthesized PrO epitaxial thin films and investigated the magnetic and electrical properties. The PrO epitaxial thin film showed metallic conduction with the resistivity minimum at 7 K and weak ferromagnetic behavior with Curie temperature (T_C) of 28 K, unlike the previous study [16], indicating that PrO is a Kondo lattice with Pr^{2+} ions. Below 5 K, a more ferromagneticlike magnetic phase was observed concomitant with an enhanced hysteresis of the anomalous Hall effect.

II. EXPERIMENTAL METHODS

PrO (001) epitaxial thin films were deposited on $YAlO_3$ (110) substrates at 250 °C in O_2 gas pressure of 5×10^{-8} Torr by pulsed laser deposition. A Pr metal (99.9%) target was irradiated by a KrF excimer laser with a fluence of 0.6 J cm^{-2} and a frequency of 10 Hz. An amorphous AlO_x capping layer was subsequently deposited on each film at room temperature to prevent surface oxidation. Typical thicknesses of the PrO

 ©2022 American Physical Society

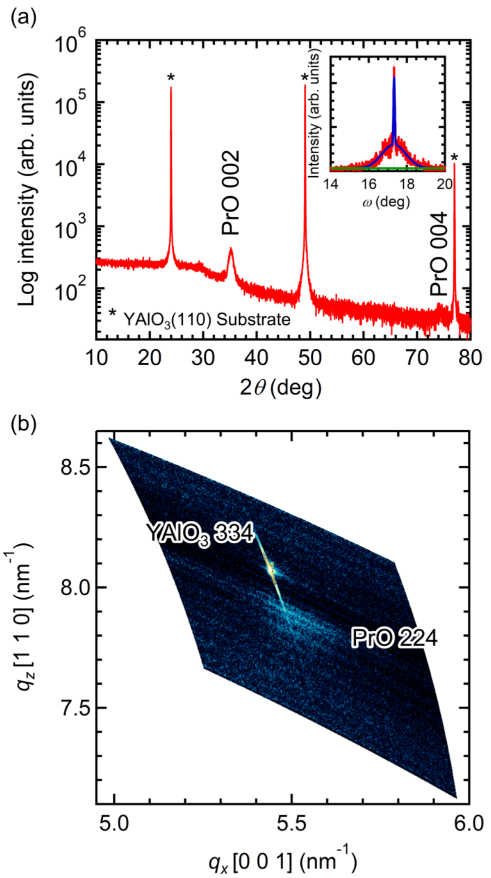

FIG. 1. (a) X-ray diffraction θ-2θ pattern and (b) reciprocal space map around the PrO 224 peak for the PrO (001) epitaxial thin film on an $YAlO_3$ (110) substrate. Inset of (a) shows the rocking curve (red) around the PrO 002 peak. The fitting curve (blue) and background (green) are also shown.

and AlO_x thin films were 10 and 6 nm, respectively. The crystal structure was evaluated by x-ray diffraction (XRD) using a four-axis diffractometer (D8 Discover, Bruker AXS). The electronic states were investigated by hard x-ray photoemission spectroscopy (HAXPES) at BL47XU of SPring-8 and x-ray absorption spectroscopy (XAS) and Pr $3d$-$4f$ resonant photoemission spectroscopy (RPES) at BL-2A of the Photon Factory. The HAXPES spectra were recorded using a ScientaR-4000 electron energy analyzer with a total energy resolution of 200 meV at a photon energy of 8 keV. The RPES spectra were recorded at various photon energies from 928 to 933 eV to cover the Pr M_5 absorption edge. The Fermi level of the samples was calibrated using a gold foil as a reference. The electrical resistivity ρ, Hall resistivity, carrier density, and mobility were measured for standard Hall bar shaped films by four-probe and Hall effect measurements using a physical property measurement system (Model 6000, Quantum Design) and a cryostat with a dilution refrigerator (Kelvinox TLM, Oxford Instruments). Anomalous Hall conductivity σ_{AHE} was calculated from the equation $\sigma_{\mathrm{AHE}} = \rho_{\mathrm{AHE}}/(\rho^2 + \rho_{\mathrm{AHE}}^2)$, where ρ_{AHE} is anomalous Hall resistivity obtained by subtracting the magnetic-field-linear component from the Hall resistivity. The magnetization measurements were performed by a superconducting quantum interference device magnetometer (MPMS-XL, Quantum Design), where the diamagnetic signals from the substrate and capping layer were subtracted. The demagnetizing field correction was made for magnetization M.

III. RESULTS AND DISCUSSION

The XRD θ-2θ pattern for the PrO thin film showed peaks of PrO $00l$ reflection and $YAlO_3$ substrate, indicating (001) epitaxial growth without any impurity phase [Fig. 1(a)]. The rocking curve around the 002 diffraction showed a superposition of a large sharp peak and a small broad peak with full width at half maximum of 0.078° and 1.50°, respectively [inset of Fig. 1(a)], indicating good crystallinity of the film and possibly a partial relaxation of the film near the surface. A spot 224 diffraction peak observed in the reciprocal space map confirmed epitaxial growth of PrO [Fig. 1(b)], where the epitaxial relationship was (001) PrO [100]//(110) $YAlO_3$ [001], similar to the other rare-earth monoxide epitaxial thin films on $YAlO_3$ (110) substrates [9,18–20,22]. The lattice constants were $a = 5.164$ Å and $c = 5.054$ Å, which are slightly larger than $a = 5.032$ Å of bulk polycrystal [16]. While the PrO epitaxial thin film was subjected to a tensile epitaxial strain, a thicker film with an almost relaxed lattice showed similar electrical and magnetic properties to those shown in Figs. S2 and S3 of the Supplemental Material [23], indicating negligible influence of the lattice strain on the properties discussed in this study.

Figure 2 shows the HAXPES spectra for the AlO_x-capped PrO thin film measured at 20 K. For the Pr $3d$ core level shown in Fig. 2(a), the spectral shape of the PrO film shows close similarity to the Pr metal rather than to Pr_2O_3 [24]. This result indicates that the chemical states (environments of $3d$ core shell) of Pr ions in PrO are close to those in Pr metal, which consist of localized $4f^2$ and itinerant $5d$ electrons as well as Pr-based intermetallics [25]. Since a similar trend has been observed for SmO [26], this seems to be a common feature in rare-earth monoxides where $5d$ electrons form the metallic conduction band. Meanwhile, a closer look reveals that the energy of the Pr $3d$ core level for PrO is located between those for Pr metal and Pr_2O_3 with nominal ionic charges of Pr^0 and Pr^{3+}, respectively [24], reflecting some ionic character of PrO (the nominal ionic charge of Pr^{2+} ions in PrO). The Pr-$5d$ derived metallic state is further confirmed by the HAXPES spectrum shown in Fig. 2(b). In the valence-band spectrum, significant density of states was clearly observed at the Fermi level, representing its metallic electronic state. Because amorphous AlO_x is an insulator with a band gap of more than 6 eV, an AlO_x capping layer does not mask the electronic structures near the Fermi level derived from the Pr $5d$ states of the buried PrO film [26]. Thus, we address the electronic structure near the Fermi level of buried PrO film by HAXPES. The observed spectra show close similarity to that of SmO [26], suggesting that the Pr ions in PrO have a $4f^2 5d^1$ electronic configuration and $5d$ electrons form the conduction band near the Fermi level.

Figure 3(a) shows the XAS spectrum for the PrO thin film taken at Pr M_4 and M_5 edges together with the theoretical spectrum calculated for the Pr^{3+} state [27]. These quite similar spectral features indicated an almost trivalent state of

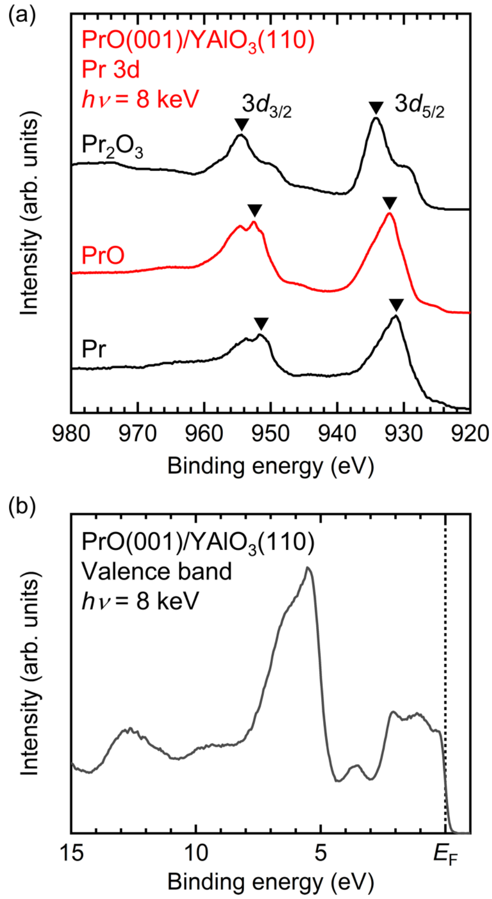

FIG. 2. HAXPES spectra of AlO_x-capped PrO epitaxial thin film for (a) Pr $3d$ core levels and (b) valence band. Spectra for Pr_2O_3 and Pr metal taken from [24] are also plotted in (a) as references.

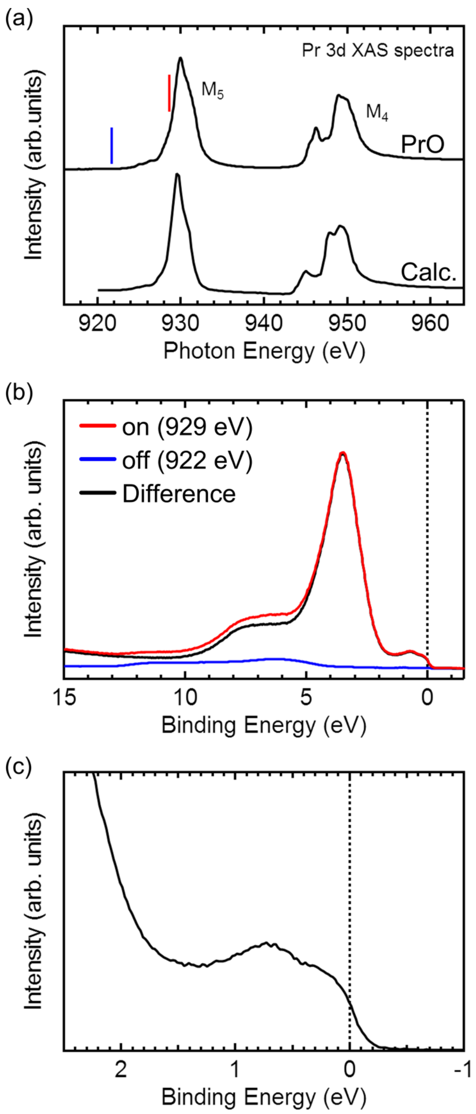

FIG. 3. (a) XAS spectra for PrO thin film around the Pr M_4 and M_5 edges, and calculated for the Pr^{3+} state after Ref. [27]. The blue and red bars indicate the photon energies used in the RPES shown in (b). (b) Valence-band RPES spectra on (929 eV) and off (922 eV) resonance and their difference. The difference spectrum is obtained by subtracting the off-resonant spectrum from the on-resonant spectrum and thus corresponds to the Pr $4f$ spectrum of PrO. (c) Magnified plot for the difference (Pr $4f$) spectrum in (b) near the Fermi level.

Pr ions in PrO, being consistent with the above-mentioned HAXPES spectrum. Figure 3(b) shows Pr $3d$-$4f$ RPES spectra taken at the corresponding photon energies for on and off resonance at the M_5 absorption edge. Clearly enhanced intensity for the on-resonance state at the Fermi level represents a non-negligible $4f$ contribution to the Fermi level [Fig. 3(c)]. Meanwhile, the much stronger on-resonance peak at the binding energy of 3.5 eV is consistent with the Pr^{3+} state, in which the majority of the $4f^2$ electrons were localized. These results indicate that the hybridization between the conduction and f electrons (c-f hybridization) is weak in PrO [Fig. 3(a)].

The PrO thin film showed metallic conduction with approximately temperature (T)-linear resistivity ρ above 7 K [Fig. 4(a)]. A kink was observed at around 30 K in the $(d\rho/dT)$-T curve shown in Fig. S4 in the Supplemental Material [23], corresponding to the magnetic phase transition mentioned below. The carrier density and the mobility at 50 mK were $2.94 \times 10^{22}\,\mathrm{cm^{-3}}$ and $2.30\,\mathrm{cm^2\,V^{-1}\,s^{-1}}$, respectively, where the former value was in good coincidence with the density of the Pr ions in PrO ($2.97 \times 10^{22}\,\mathrm{cm^{-3}}$), representing the fully itinerant $5d^1$ electrons of the Pr ions. Below 7 K, the resistivity logarithmically increased with decreasing temperature and became almost constant for 0.02–0.2 K, as a manifestation of typical Kondo effect [Fig. 4(b)]. A similar behavior was observed for a thicker PrO thin film with a smaller resistivity owing to the smaller contribution of scattering at the surface and film/substrate interface shown in Fig. S2 [23], indicating that the Kondo effect was induced by an intrinsic origin. The resistivity minimum was robust against the external magnetic field of 9 T with small negative magnetoresistance like SmO [18], in spite of the unclear origin of the robustness. This ρ-T curve was well fitted to the following empirical equation of the Kondo effect [28–30],

$$\rho = \rho_b + \frac{\rho_0}{2}\left\{1 - \frac{\ln\left[\left(T^2 + T_W^2\right)/T_K^2\right]^{1/2}}{\pi\left[S(S+1)\right]^{1/2}}\right\} + bT^n, \qquad (1)$$

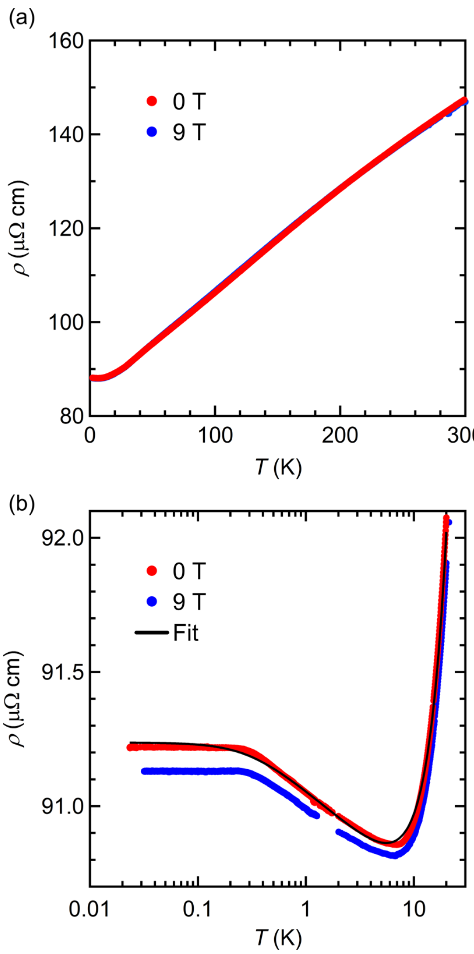

FIG. 4. Temperature dependence of electrical resistivity ρ in the temperature ranges of (a) 2–300 K and (b) 0.02–20 K under out of the plane magnetic field of 0 and 9 T for PrO epitaxial thin film. The black line denotes fitting result for ρ at 0 T in the temperature range 0.02–20 K by Eq. (1). The discontinuous data at around 1 K were caused by the different measurement systems.

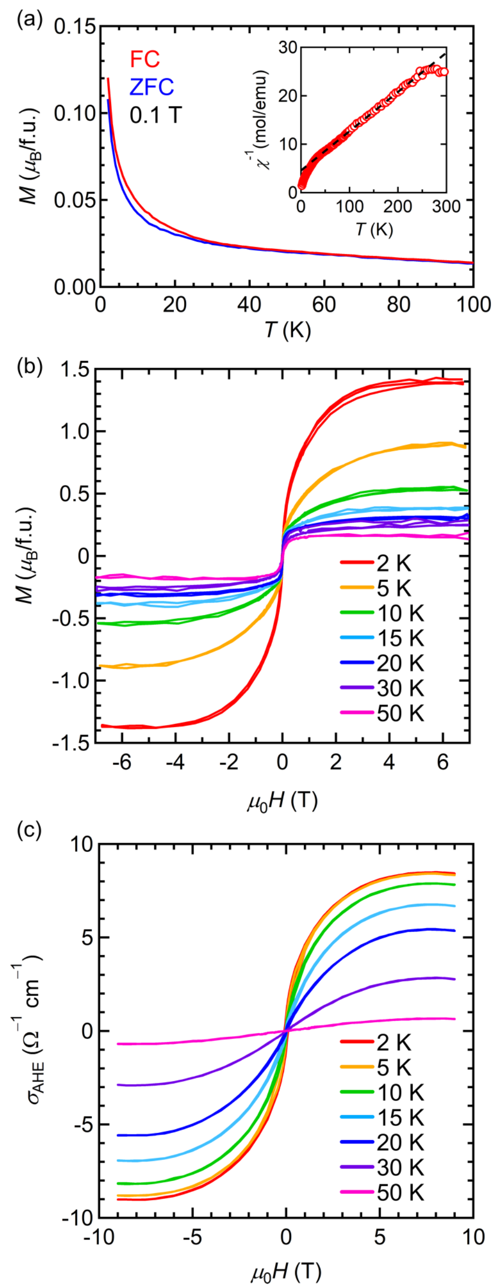

FIG. 5. (a) Temperature dependence of magnetization M at 0.1 T in field cooling (FC: red) and zero field cooling (ZFC: blue). Inset shows temperature dependence of inverse susceptibility for the FC data, where the dashed line denotes linear fitting for the high-temperature region. (b,c) Magnetic field dependence of (b) M and (c) anomalous Hall conductivity σ_{AHE} for PrO epitaxial thin film at various temperatures. Magnetic field was applied along the out of plane direction.

where ρ_b is residual resistivity, ρ_0 is the unitarity limit, $\ln(T_W/T_K) = -\pi[S(S+1)]^{1/2}$, T_W is the effective RKKY interaction strength, T_K is the Kondo temperature, S is the spin of the magnetic ion, and b is the coefficient for the high-temperature metallic region with a T^n dependence (see Supplemental Material for details on the fitting procedure [23]). The fitting result as well as the non-negligible $c-f$ hybridization observed in RPES indicated that the PrO thin film is a Kondo lattice with $T_K = 1.3$ K [Fig. 4(b)]. The absence of rapid decrease in resistivity at lower temperature than the local resistivity minimum is a common feature for Kondo lattices with weak c-f hybridization [31], as also seen in other Pr-based Kondo lattices such as Pr_2Ir_2O [5].

In the temperature dependence of M, the field-cooled (FC) and zero field cooled (ZFC) curves showed rapid increase below ~30 K [Fig. 5(a)], corresponding to the kink in the $(d\rho/dT)$-T curve shown in Fig. S4 [23]. Unchanged temperature of the kink at 0 and 9 T ruled out a possible formation of spin glass, indicating the presence of a long-range magnetic ordering. Indeed, ferromagnetic hysteresis was observed in magnetization curves below 20 K [Figs. 5(b) and 6]. The anomalous Hall conductivity σ_{AHE} also showed the ferromagnetic hysteresis in the same temperature range [Figs. 5(c) and 6]. The Curie temperature (T_C) was estimated to be 27.8 K from a linear fit for the temperature dependence of the magnetization difference between the FC and ZFC curves (ΔM) due to the small magnetization shown in Fig. S5 [23]. On the other hand, the Weiss temperature θ_W was determined

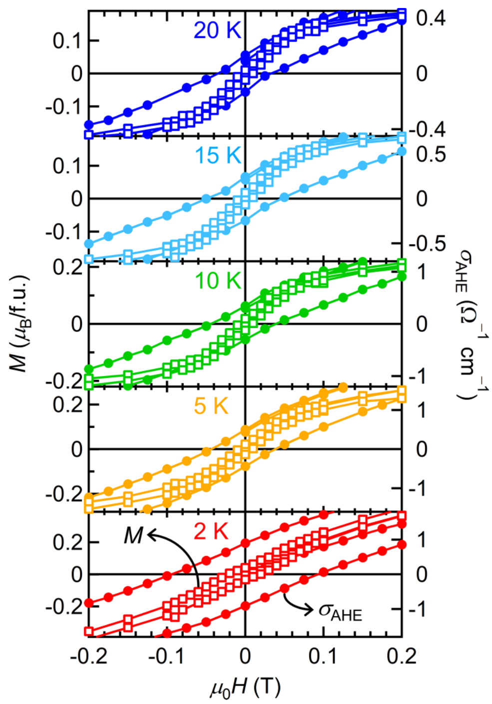

FIG. 6. Magnetic field dependence of magnetization M (open square) and anomalous Hall conductivity σ_{AHE} (filled circle) in the low magnetic field region at various temperatures.

to be −57 K from the Curie-Weiss plot [inset of Fig. 5(a)]. While the renormalization group theory predicted negative θ_W in the same order as T_K [32], $|\theta_W|$ was one order of magnitude higher than T_K for the PrO thin film, indicating enhancement by antiferromagnetic interaction as seen in antiferromagnetic Kondo lattices [33,34]. Taking into account the large negative value of θ_W and small hysteresis, PrO is regarded as a weak ferromagnet contrary to the previous study [16]. $|\theta_W|$ being larger than the magnetic transition temperature indicates that the interaction between the first nearest neighbors is stronger than that between the second nearest neighbors [35], probably due to the short Pr-Pr ionic distance in PrO. Accordingly, we suppose there is a canted antiferromagnetic ordering with a small net magnetization for the weak ferromagnetism in PrO. Because of the shorter cationic distance than that of the other Pr*Ch*, not only the RKKY interaction but also the $4f$-$4f$ exchange interaction and superexchange interaction influence the magnetism in PrO, where the $4f$-$4f$ exchange interaction may be mediated by virtual excitation to the $5d$ orbital as in EuO [36]. Considering a weak ferromagnetism in PrN without itinerant electrons [15], such local exchange interactions played a crucial role for the long-range magnetic ordering in contrast with other Pr*Ch*. In addition, the clearly open magnetic hysteresis of PrO in contrast with no measurable hysteresis of PrN down to 4 K [15] indicated a significant role of ferromagnetic RKKY interaction.

Rapid increase in saturation magnetization M_s from 5 to 2 K indicated emergence of another magnetic phase below 5 K shown in Figs. 5(b) and S6(a) [23]. The magnetic phase was considered to be weak ferromagnetic but more ferromagneticlike than the higher-temperature phase, taking into account still significantly smaller M_s of 1.4 μ_B/f.u. at 2 K than the theoretical saturation magnetic moment 3.20 μ_B for a Pr^{3+} ion with a $4f^2$ electronic configuration. Such a small M_s was also reported for NdO epitaxial thin films [9], attributed to crystal field splitting. At 2 K, the coercive force H_c became much larger for σ_{AHE} than for M shown in Figs. 6 and S6(b) [23]. The much larger hysteresis of σ_{AHE} at 2 K suggested a nontrivial magnetic structure like that of Pr_2Ir_2O [37], presumably attributed to the competition between the $4f$-$4f$ exchange interaction, superexchange interaction, and RKKY interaction.

IV. SUMMARY

In summary, we succeeded in synthesis of PrO epitaxial thin films. The PrO epitaxial thin films with a $4f^25d^1$ electronic configuration showed weak ferromagnetic behavior with $T_C = 28$ K, reflecting the significant contribution of the $4f$-$4f$ exchange interaction due to the short Pr-Pr distance. Below 5 K, a more ferromagneticlike phase emerged probably because of the ferromagnetic RKKY interaction, concomitant with much larger hysteresis of the anomalous Hall effect than that of magnetization, suggesting competing magnetic ordering. Simple rocksalt-type PrO is a prototypical Kondo lattice that can provide a rich magnetic phase diagram.

ACKNOWLEDGMENTS

We would like to thank Professor N. Shibata and Professor T. Koretsune of Tohoku University for fruitful comments. The HAXPES experiments were performed at BL47XU (Proposal No. 2019B2148). This work was in part supported by JSPS-KAKENHI (Grants No. 18H03872, No. 18K18935, No. 19K15440, No. 20H02704, No. 21H05008) and the Mitsubishi Foundation.

[1] H. V. Löhneysen, A. Rosch, M. Vojta, and P. Wölfle, Rev. Mod. Phys. **79**, 1015 (2007).
[2] K. Satoh, T. Fujita, Y. Maeno, Y. Onuki, and T. Komatsubara, J. Phys. Soc. Jpn. **58**, 1012 (1989).
[3] Y. F. Yang, Z. Fisk, H. O. Lee, J. D. Thompson, and D. Pines, Nature (London) **454**, 611 (2008).
[4] A. Sakai, K. Kuga, and S. Nakatsuji, J. Phys. Soc. Jpn. **81**, 083702 (2012).
[5] S. Nakatsuji, Y. Machida, Y. Maeno, T. Tayama, T. Sakakibara, J. van Duijn, L. Balicas, J. N. Millican, R. T. Macaluso, and J. Y. Chan, Phys. Rev. Lett. **96**, 087204 (2006).
[6] A. Tsuruta and K. Miyake, J. Phys. Soc. Jpn. **84**, 114714 (2015).
[7] H. Sato, H. Sugawara, T. Namiki, S. R. Saha, S. Osaki, T. D. Matsuda, Y. Aoki, Y. Inada, H. Shishido, R. Settai, and Y. Onuki, J. Phys.: Condens. Matter **15**, S2063 (2003).

[8] T. Onimaru and H. Kusunose, J. Phys. Soc. Jpn. **85**, 082002 (2016).
[9] D. Saito, K. Kaminaga, D. Oka, and T. Fukumura, Phys. Rev. Mater. **3**, 064407 (2019).
[10] G. Guntherodt, Phys. Cond. Matter **18**, 37 (1974).
[11] C. G. Duan, R. F. Sabirianov, W. N. Mei, P. A. Dowben, S. S. Jaswal, and E. Y. Tsymbal, J. Phys.: Condens. Matter **19**, 315220 (2007).
[12] T. Kasuya, J. Alloys Compd. **192**, 11 (1993).
[13] S. K. Hasanain, R. P. Guertin, K. Westerholt, M. Guyot, and S. Foner, Phys. Rev. B **24**, 5165 (1981).
[14] E. Bucher, K. Andres, F. J. Di Salvo, J. P. Maita, A. C. Gossard, A. S. Cooper, and G. W. Hull, Phys. Rev. B **11**, 500 (1975).
[15] D. P. Schumacher and W. E. Wallace, J. Appl. Phys. **36**, 984 (1965).
[16] G. Krill, M. F. Ravet, J. P. Kappler, L. Abadli, J. M. Leger, N. Yacoubi, and C. Loriers, Solid State Commun. **33**, 351 (1980).
[17] K. Kaminaga, R. Sei, K. Hayashi, N. Happo, H. Tajiri, D. Oka, T. Fukumura, and T. Hasegawa, Appl. Phys. Lett. **108**, 122102 (2016).
[18] Y. Uchida, K. Kaminaga, T. Fukumura, and T. Hasegawa, Phys. Rev. B **95**, 125111 (2017).
[19] K. Kaminaga, D. Oka, T. Hasegawa, and T. Fukumura, J. Am. Chem. Soc. **140**, 6754 (2018).
[20] T. Yamamoto, K. Kaminaga, D. Saito, D. Oka, and T. Fukumura, Appl. Phys. Lett. **114**, 162104 (2019).
[21] T. Yamamoto, K. Kaminaga, D. Saito, D. Oka, and T. Fukumura, Appl. Phys. Lett. **117**, 052402 (2020).
[22] T. Yamasaki, K. Ueno, A. Tsukazaki, T. Fukumura, and M. Kawasaki, Appl. Phys. Lett. **98**, 082116 (2011).
[23] See Supplemental Material at http://link.aps.org/supplemental/10.1103/PhysRevB.105.014442 for fitting procedure of Kondo effect, and detailed data of electrical and magnetic properties of PrO thin films.
[24] S. Lütkehoff, M. Neumann, and A. Slebarski, Phys. Rev. B **52**, 13808 (1995).
[25] A. Yamasaki, S. Imada, A. Sekiyama, M. Tsunekawa, C. Dallera, L. Braicovich, T. L. Lee, H. Sugawara, H. Sato, R. Settai, Y. Onuki, and S. Suga, J. Phys. Soc. Jpn. **74**, 2045 (2005).
[26] S. Sakamoto, K. Kaminaga, D. Oka, R. Yukawa, M. Horio, Y. Yokoyama, K. Yamamoto, K. Takubo, Y. Nonaka, K. Koshiishi, M. Kobayashi, A. Tanaka, A. Yasui, E. Ikenaga, H. Wadati, H. Kumigashira, T. Fukumura, and A. Fujimori, Phys. Rev. Mater. **4**, 095001 (2020).
[27] B. T. Thole, G. van der Laan, J. C. Fuggle, G. A. Sawatzky, R. C. Karnatak, and J.-M. Esteva, Phys. Rev. B **32**, 5107 (1985).
[28] T. Sekitani, M. Naito, and N. Miura, Phys. Rev. B **67**, 174503 (2003).
[29] S. Barua, M. C. Hatnean, M. R. Lees, and G. Balakrishnan, Sci. Rep. **7**, 10964 (2017).
[30] D. R. Hamann, Phys. Rev. **158**, 570 (1967).
[31] O. Howczak, J. Kaczmarczyk, and J. Spałek, Phys. Status Solidi B **250**, 609 (2013).
[32] K. G. Wilson, Rev. Mod. Phys. **47**, 773 (1975).
[33] D. T. Adroja, B. D. Rainford, L. Menon, and S. K. Malik, J. Phys.: Condens. Matter **9**, 4743 (1997).
[34] R. Pietri and B. Andraka, Phys. Rev. B **66**, 224421 (2002).
[35] S. Chikazumi, *Physics of Ferromagnetism*, 2nd ed. (Oxford University Press, Oxford, 1997).
[36] M. Matsubara, Appl. Sci. **9**, 948 (2019).
[37] Y. Machida, S. Nakatsuji, S. Onoda, T. Tayama, and T. Sakakibara, Nature (London) **463**, 210 (2010).